Three-Dimensional Sharp Corner Displacement Functions for Bodies of Revolution

C. S. Huang[1]
Department of Civil Engineering,
National Chiao Tung University,
1001 Ta-Hsueh Road,
Hsinchu, Taiwan, ROC
e-mail: cshuang@mail.nctu.edu.tw

A. W. Leissa
Department of Mechanical Engineering,
Colorado State University,
Fort Collins, CO 80523

Sharp corner displacement functions have been well used in the past to accelerate the numerical solutions of two-dimensional free vibration problems, such as plates, to obtain accurate frequencies and mode shapes. The present analysis derives such functions for three-dimensional (3D) bodies of revolution where a sharp boundary discontinuity is present (e.g., a stepped shaft, or a circumferential V notch), undergoing arbitrary modes of deformation. The 3D equations of equilibrium in terms of displacement components, expressed in cylindrical coordinates, are transformed to a new coordinate system having its origin at the vertex of the corner. An asymptotic analysis in the vicinity of the sharp corner reduces the equations to a set of coupled, ordinary differential equations with variable coefficients. By a suitable transformation of variables the equations are simplified to a set of equations with constant coefficients. These are solved, the boundary conditions along the intersecting corner faces are applied, and the resulting eigenvalue problems are solved for the characteristic equations and corner functions.
[DOI: 10.1115/1.2178358]

Introduction

Williams [1–3] showed a typical procedure to determine singular corner functions for the two-dimensional (2D) problems of plane elasticity and classical plate bending theory. These analyses have been used for a half century to determine stresses in the vicinity of sharp corners. The corner functions are either Airy stress functions (plane elasticity) or transverse displacement functions (plate bending) which are exact solutions of the partial differential equations of equilibrium. Satisfying the boundary conditions along the two radial edges which form the sharp corner results in an eigenvalue problem. Determining the roots (eigenvalues) of the characteristic equation and substituting them back into the boundary conditions yields the corner functions (eigenfunctions). Their second derivatives are the stresses. Extending Williams' works, numerous researchers used different solution schemes to determine the characteristic equations for a thin wedge consisted of two materials [4–7] or for three-dimensional elastic problems [8–10]. Nevertheless, no corner functions were explicitly provided in these works.

Subsequently, the corner functions themselves were used for plate vibration problems which are solved by the well-known Ritz [11,12] method. To a series of smooth algebraic polynomials for the transverse displacement (w) is added a series of corner functions. The latter accelerate the convergence of the solution for the desired free vibration frequencies and mode shapes because they represent the behavior well in the vicinity of a sharp corner. Because of the singularities there, the algebraic polynomials do not. This approach has been used to obtain accurate (i.e., almost exact) frequencies and mode shapes for sectorial plates [13], circular plates with V notches or sharp radial cracks [14], cantilevered skewed plates [15], and rhombic plates [16]. Three sets of corner functions (transverse displacement and two bending rotations) were also derived for 2D Midlin plate theory [17] and used with algebraic polynomials to analyze the vibrations of thick, cantilevered skewed plates [18]. It was found for many of the plate configurations, thin and thick, that the use of corner functions to supplement the algebraic polynomials greatly accelerated the convergence of solutions. In some cases, without them, accurate frequencies could not be reasonably achieved.

Corner functions were used not only in the Ritz method but also in other numerical approaches. In a finite element approach, Yosibash and Schiff [19] developed a singular superelement by using corner functions for plane elasticity and evaluated the stress intensity factors for a V-notched plate under different in-plane loading. The singular superelement overcomes the difficulties in accurately determining the stresses in the neighborhood of the tip of the V notch by using a traditional finite element approach. Corner functions or parts of corner functions were also used in the mesh-free Galerkin method [20,21] and a partition of unity method [22] to approximate crack tip displacement field and to determine intensity factors.

In recent years, because of the increase in computer speeds and storage capability, it has been possible to obtain accurate solutions for three-dimensional (3D) problems, especially for bodies of revolution, using algebraic polynomials for the three displacement components. For example, accurate frequencies have been achieved for cylinders [23], hollow cones [24], and spheres [25,26]. Frequencies for a fixed-free cylinder were found to converge much slower than for a free-free one [23], due to the stress singularities at the fixed end, and the lack of corner functions. For such shapes there were no abrupt changes in the boundary shapes. However, shapes with abrupt changes (e.g., a stepped circular shaft or a cone segment bonded to a circular cylinder (Fig. 1)) cause stress singularities, and adding suitable corner functions to the analysis can be essential. The purpose of this paper is to derive these functions.

One analysis of the stresses in the vicinity of boundary discontinuities was summarized by Zak [27] in a Brief Note here four decades ago, for the special case of axisymmetric loading. His analysis used a stress function presented by Love [28] for axisymmetric problems.

The present work approaches the 3D elasticity problem from the standpoint of displacements, which will ultimately be the corner functions sought. Beginning with the 3D equations of equilib-

[1]To whom correspondence should be addressed.

Contributed by the Applied Mechanics Division of ASME for publication in the Journal of Applied Mechanics. Manuscript received July 26, 2004; final manuscript received April 26, 2005. Review conducted by H. D. Espinosa. Discussion on the paper should be addressed to the Editor, Prof. Robert M. McMeeking, Journal of Applied Mechanics, Department of Mechanical and Environmental Engineering, University of California – Santa Barbara, Santa Barbara, CA 93106-5070, and will be accepted until four months after final publication of the paper itself in the ASME Journal of Applied Mechanics.

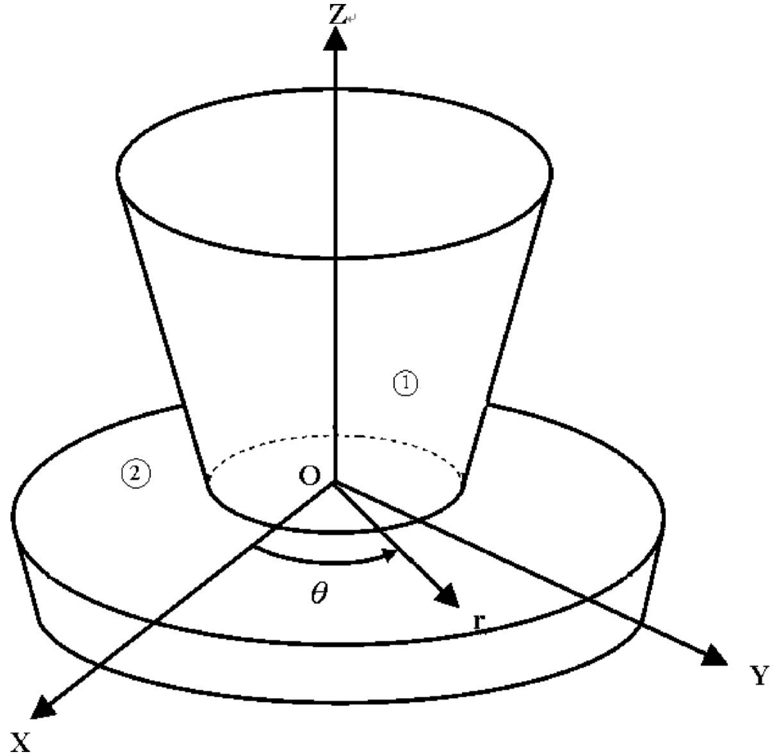

Fig. 1 Body of revolution with a sharp corner boundary discontinuity

rium for elastic bodies of revolution, capable of arbitrary displacements (including axisymmetric ones as a special case), expressed in cylindrical coordinates, they are transformed to a new axis system having its origin at the sharp corner. An asymptotic analysis in the vicinity of the sharp corner reduces the equations to a set of coupled, ordinary differential equations with variable coefficients. By a suitable transformation of variables the equations are simplified to a set of equations with constant coefficients. These are solved, the boundary conditions along the intersecting corner faces are applied, and the resulting eigenvalue problems are solved for the characteristic equations and corner functions.

Equilibrium Equations for a Sharp Corner

The 3D equations of equilibrium, expressed in terms of cylindrical coordinates (r,θ,z), are (cf. [29])

$$\sigma_{r,r}+\frac{\tau_{r\theta,\theta}}{r}+\tau_{rz,z}+\frac{\sigma_r-\sigma_\theta}{r}=0 \tag{1a}$$

$$\tau_{r\theta,r}+\frac{\sigma_{\theta,\theta}}{r}+\tau_{\theta z,z}+\frac{2\tau_{r\theta}}{r}=0 \tag{1b}$$

$$\tau_{rz,r}+\frac{\tau_{\theta z,\theta}}{r}+\sigma_{z,z}+\frac{\tau_{rz}}{r}=0 \tag{1c}$$

where the σ_i and τ_{ij} are normal and shear stresses, respectively, and the subscript ",β" denotes the differential with respect to the independent variable β. To express them, instead, in terms of displacement components, one uses the stress-strain equations for an isotropic material

$$\sigma_i=\bar{\lambda}e+2G\varepsilon_i, \quad \tau_{ij}=G\gamma_{ij} \tag{2}$$

where the ε_i and γ_{ij} are normal and shear strains, respectively, and

$$e=\varepsilon_r+\varepsilon_\theta+\varepsilon_z, \quad G=\frac{E}{2(1+\upsilon)}, \quad \bar{\lambda}=\frac{2\upsilon G}{1-2\upsilon} \tag{3}$$

where $\bar{\lambda}$ is the Lamé parameter; G, E, and υ are the shear modulus, Young's modulus, and Poisson's ratio for the material, respectively, and the strain-displacement relations (cf. [29])

$$\varepsilon_r=u_{,r}, \quad \varepsilon_\theta=\frac{1}{r}(v_{,\theta}+u), \quad \varepsilon_z=w_{,z}, \quad \gamma_{r\theta}=\frac{u_{,\theta}}{r}+v_{,r}-\frac{v}{r},$$
$$\gamma_{rz}=w_{,r}+u_{,z}, \quad \gamma_{\theta z}=v_{,z}+\frac{w_{,\theta}}{r} \tag{4}$$

where u, v, and w are displacement components in the r, θ, and z directions, respectively. Substituting Eqs. (2)–(4) into Eq. (1), one obtains

$$2(1-\upsilon)u_{,rr}+\frac{2(1-\upsilon)}{r}u_{,r}-2(1-\upsilon)\frac{u}{r^2}+\frac{1-2\upsilon}{r^2}u_{,\theta\theta}+(1-2\upsilon)u_{,zz}$$
$$+\frac{1}{r}v_{,r\theta}-\frac{3-4\upsilon}{r^2}v_{,\theta}+w_{,rz}=0 \tag{5a}$$

$$\frac{1}{r}u_{,r\theta}+\frac{3-4\upsilon}{r^2}u_{,\theta}+(1-2\upsilon)v_{,rr}+(1-2\upsilon)\frac{v_{,r}}{r}-(1-2\upsilon)\frac{v}{r^2}$$
$$+\frac{2(1-\upsilon)}{r^2}v_{,\theta\theta}+(1-2\upsilon)v_{,zz}+\frac{1}{r}w_{,\theta z}=0 \tag{5b}$$

$$u_{,rz}+\frac{u_{,z}}{r}+\frac{v_{,\theta z}}{r}+2(1-\upsilon)w_{,zz}+(1-2\upsilon)w_{,rr}+\frac{1-2\upsilon}{r}w_{,r}$$
$$+\frac{1-2\upsilon}{r^2}w_{,\theta\theta}=0 \tag{5c}$$

These equations are also found, for example, in the paper by Chaudhuri and Xie [30].

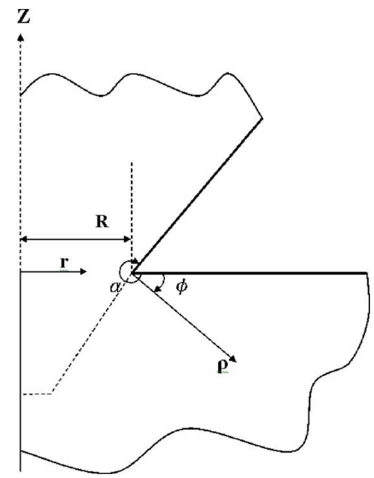

Fig. 2 Cylindrical (r,z) and sharp corner (ρ,ϕ) coordinates

Because solutions of Eqs. (5) will be applied to bodies of revolution subjected to arbitrary static or dynamic loads, it is propitious to assume them as Fourier components in θ

$$u=\sum_{n=0,1} U_n(r,z)\cos n\theta, \quad v=\sum_{n=0,1} V_n(r,z)\sin n\theta \text{ and} \tag{6}$$

$$w=\sum_{n=0,1} W_n(r,z)\cos n\theta$$

Substituting them into Eqs. (5) yields

$$\begin{aligned}&2(1-\upsilon)U_{n,rr}+\frac{2(1-\upsilon)}{r}U_{n,r}-[2(1-\upsilon)+n^2(1-2\upsilon)]\frac{U_n}{r^2}\\&\quad+(1-2\upsilon)U_{n,zz}+\frac{n}{r}V_{n,r}-\frac{n(3-4\upsilon)}{r^2}V_n+W_{n,rz}=0\end{aligned} \tag{7a}$$

$$\begin{aligned}&-\frac{n}{r}U_{n,r}-\frac{(3-4\upsilon)n}{r^2}U_n+(1-2\upsilon)V_{n,rr}+\frac{1-2\upsilon}{r}V_{n,r}\\&\quad-[(1-2\upsilon)+2n^2(1-\upsilon)]\frac{V_n}{r^2}+(1-2\upsilon)V_{n,zz}-\frac{n}{r}W_{n,z}=0\end{aligned} \tag{7b}$$

$$\begin{aligned}&U_{n,rz}+\frac{1}{r}U_{n,z}+\frac{n}{r}V_{n,z}+2(1-\upsilon)W_{n,zz}+(1-2\upsilon)W_{n,rr}+\frac{1-2\upsilon}{r}W_{n,r}\\&\quad-\frac{n^2(1-2\upsilon)}{r^2}W_n=0\end{aligned} \tag{7c}$$

To investigate the stress singularities at a sharp corner along the circumference of the body, (r, z) coordinates are transformed to (ρ,ϕ) coordinates as shown in Fig. 2. The relations between the two coordinate systems are

$$\rho=\sqrt{(r-R)^2+z^2}, \quad \phi=\tan^{-1}\left(\frac{-z}{r-R}\right) \tag{8a}$$

and

$$r-R=\rho\cos\phi, \quad z=-\rho\sin\phi. \tag{8b}$$

Utilizing Eqs. (8) with chain rule differentiation, Eqs. (7) become

$$\begin{aligned}&[2(1-\upsilon)\cos^2\phi+(1-2\upsilon)\sin^2\phi]U_{n,\rho\rho}\\&\quad+\left[2(1-\upsilon)\left(\frac{\sin^2\phi}{\rho}+\frac{\cos\phi}{\rho\cos\phi+R}\right)+(1-2\upsilon)\frac{\cos^2\phi}{\rho}\right]U_{n,\rho}\\&\quad-\frac{\sin 2\phi}{\rho}U_{n,\rho\phi}-\frac{2(1-\upsilon)+(1-2\upsilon)n^2}{(\rho\cos\phi+R)^2}U_n\\&\quad+\left[2(1-\upsilon)\frac{\sin^2\phi}{\rho^2}+(1-2\upsilon)\frac{\cos^2\phi}{\rho^2}\right]U_{n,\phi\phi}\\&\quad+\left[-\frac{2(1-\upsilon)}{\rho\cos\phi+R}\frac{\sin\phi}{\rho}+\frac{\sin 2\phi}{\rho^2}\right]U_{n,\phi}+\frac{n\cos\phi}{\rho\cos\phi+R}V_{n,\rho}\\&\quad-\frac{n\sin\phi}{\rho(\rho\cos\phi+R)}V_{n,\phi}-\frac{n(3-4\upsilon)}{(\rho\cos\phi+R)^2}V_n-\sin\phi\cos\phi W_{n,\rho\rho}\\&\quad+\frac{\sin\phi\cos\phi}{\rho}W_{n,\rho}-\frac{\cos 2\phi}{\rho}W_{n,\rho\phi}\\&\quad+\frac{\sin\phi\cos\phi}{\rho^2}W_{n,\phi\phi}+\frac{\cos 2\phi}{\rho^2}W_{n,\phi}=0\end{aligned} \tag{9a}$$

$$\begin{aligned}&-\frac{n}{\rho\cos\phi+R}\left(\cos\phi U_{n,\rho}-\frac{\sin\phi}{\rho}U_{n,\phi}\right)-\frac{n(3-4\upsilon)}{(\rho\cos\phi+R)^2}U_n\\&\quad+(1-2\upsilon)V_{n,\rho\rho}+(1-2\upsilon)\left(\frac{1}{\rho}+\frac{\cos\phi}{\rho\cos\phi+R}\right)V_{n,\phi}\\&\quad+\frac{1-2\upsilon}{\rho^2}V_{n,\phi\phi}-\frac{1-2\upsilon}{\rho\cos\phi+R}\frac{\sin\phi}{\rho}V_{n,\phi}\\&\quad-\frac{(1-2\upsilon)+2n^2(1-\upsilon)}{(\rho\cos\phi+R)^2}V_n+\frac{n}{\rho\cos\phi+R}\\&\quad\times\left(\sin\phi W_{n,\rho}+\frac{\cos\phi}{\rho}W_{n,\phi}\right)=0\end{aligned} \tag{9b}$$

$$\begin{aligned}&-\sin\phi\cos\phi U_{n,\rho\rho}-\frac{\cos 2\phi}{\rho}U_{n,\rho\phi}\\&\quad+\left(\frac{\sin\phi\cos\phi}{\rho}-\frac{\sin\phi}{\rho\cos\phi+R}\right)U_{n,\rho}\\&\quad+\frac{\sin\phi\cos\phi}{\rho^2}U_{n,\phi\phi}+\left(\frac{\cos 2\phi}{\rho^2}-\frac{\cos\phi}{\rho(\rho\cos\phi+R)}\right)U_{n,\phi}\\&\quad-\frac{n}{\rho\cos\phi+R}\left(\sin\phi V_{n,\rho}+\frac{\cos\phi}{\rho}V_{n,\phi}\right)\\&\quad+[2(1-\upsilon)\sin^2\phi+(1-2\upsilon)\cos^2\phi]W_{n,\rho\rho}+\frac{\sin 2\phi}{\rho}W_{n,\rho\phi}\\&\quad+\left[2(1-\upsilon)\frac{\cos^2\phi}{\rho}+(1-2\upsilon)\left(\frac{\sin^2\phi}{\rho}+\frac{\cos\phi}{\rho\cos\phi+R}\right)\right]W_{n,\rho}\\&\quad+[2(1-\upsilon)\cos^2\phi+(1-2\upsilon)\sin^2\phi]\frac{1}{\rho^2}W_{n,\phi\phi}\\&\quad+\left[-2(1-\upsilon)\frac{\sin 2\phi}{\rho^2}+(1-2\upsilon)\left(\frac{\sin 2\phi}{\rho^2}\right.\right.\\&\quad\left.\left.-\frac{\sin\phi}{\rho(\rho\cos\phi+R)}\right)\right]W_{n,\phi}-\frac{n^2(1-2\upsilon)}{(\rho\cos\phi+R)^2}W_n=0\end{aligned} \tag{9c}$$

Now assume

$$U_n(\rho,\phi)=\sum_{m=0,1}^{\infty}\rho^{\lambda+m}\hat{U}_{nm}(\phi),$$

$$V_n(\rho,\phi)=\sum_{m=0,1}^{\infty}\rho^{\lambda+m}\hat{V}_{nm}(\phi),$$

$$W_n(\rho,\phi)=\sum_{m=0,1}^{\infty}\rho^{\lambda+m}\hat{W}_{nm}(\phi), \tag{10}$$

where λ is a yet-undetermined parameter, which can be a complex number. The real part of λ should be positive to make displacement components finite at $\rho=0$. Multiplying through Eqs. (9) by $(\rho\cos\phi+R)^2$, substituting Eqs. (10), and retaining only those terms with the lowest degree of ρ, one obtains the following equations to describe the behavior at the sharp corner:

$$[\lambda(\lambda-1)\cos^2\phi+\lambda^2(1-2\upsilon)+\lambda\sin^2\phi]\hat{U}_{n0}-(\lambda-1)\sin 2\phi\hat{U}_{n0,\phi}+(\sin^2\phi+1-2\upsilon)\hat{U}_{n0,\phi\phi}+\sin\phi\cos\phi\hat{W}_{n0,\phi\phi}+(1-\lambda)\cos 2\phi\hat{W}_{n0,\phi}+\lambda(2-\lambda)\sin\phi\cos\phi\hat{W}_{n0}=0 \tag{11a}$$

$$\hat{V}_{n0,\phi\phi}+\lambda^2\hat{V}_{n0}=0 \tag{11b}$$

$$\lambda(2-\lambda)\sin\phi\cos\phi\hat{U}_{n0}+(1-\lambda)\cos 2\phi\hat{U}_{n0,\phi}+\sin\phi\cos\phi\hat{U}_{n0,\phi\phi}+[\lambda(\lambda-1)\sin^2\phi+\lambda^2(1-2\upsilon)+\lambda\cos^2\phi]\hat{W}_{n0}+(\lambda-1)\sin 2\phi\hat{W}_{n0,\phi}+(\cos^2\phi+1-2\upsilon)\hat{W}_{n0,\phi\phi}=0 \tag{11c}$$

Equations (11) are independent of n, which means that the stress singularities at ρ approaching to zero are expected to be the same as those for axisymmetric problems ($n=0$).

The solution of Eq. (11b) is simply

$$\hat{V}_{n0}=A_1\cos\lambda\phi+A_2\sin\lambda\phi, \tag{12}$$

where A_1 and A_2 are coefficients to be determined from boundary conditions. Equations (11a) and (11c) are two coupled ordinary differential equations with variable coefficients.

Equations (11a) and (11c) are simplified to a set of equations with constant coefficients by the following transformation. Define new functions $\bar{U}_{n0}$ and $\bar{W}_{n0}$ such that

$$\hat{U}_{n0}(\phi)=\cos\phi\bar{U}_{n0}(\phi)-\sin\phi\bar{W}_{n0}(\phi) \tag{13a}$$

$$\hat{W}_{n0}(\phi)=-\sin\phi\bar{U}_{n0}(\phi)-\cos\phi\bar{W}_{n0}(\phi) \tag{13b}$$

Substituting Eqs. (13a) and (13b) into Eqs. (11a) and (11c) with careful rearrangement yields

$$(1-2\upsilon)\cos\phi\bar{U}_{n0,\phi\phi}-(3+\lambda-4\upsilon)\sin\phi\bar{U}_{n0,\phi}+2(\lambda^2-1)(1-\upsilon)\cos\phi\bar{U}_{n0}-2(1-\upsilon)\sin\phi\bar{W}_{n0,\phi\phi}+(-3+\lambda+4\upsilon)\cos\phi\bar{W}_{n0,\phi}+(1-\lambda^2)(1-2\upsilon)\sin\phi\bar{W}_{n0}=0 \tag{14a}$$

$$-(1-2\upsilon)\sin\phi\bar{U}_{n0,\phi\phi}-(3+\lambda-4\upsilon)\cos\phi\bar{U}_{n0,\phi}-2(\lambda^2-1)(1-\upsilon)\sin\phi\bar{U}_{n0}-2(1-\upsilon)\cos\phi\bar{W}_{n0,\phi\phi}-(-3+\lambda+4\upsilon)\sin\phi\bar{W}_{n0,\phi}+(1-\lambda^2)(1-2\upsilon)\cos\phi\bar{W}_{n0}=0 \tag{14b}$$

Multiplying Eq. (14a) by $\cos\phi$, and subtracting Eq. (14b) multiplied by $\sin\phi$ yields

$$(1-2\upsilon)\bar{U}_{n0,\phi\phi}+2(\lambda^2-1)(1-\upsilon)\bar{U}_{n0}+(-3+\lambda+4\upsilon)\bar{W}_{n0,\phi}=0 \tag{15a}$$

Similarly, summing Eq. (14a) multiplied by $\sin\phi$ and Eq. (14b) multiplied by $\cos\phi$ yields

$$-(3+\lambda-4\upsilon)\bar{U}_{n0,\phi}-2(1-\upsilon)\bar{W}_{n0,\phi\phi}+(1-\lambda^2)(1-2\upsilon)\bar{W}_{n0}=0 \tag{15b}$$

Thus, Eqs. (15a) and (15b) are two coupled ordinary differential equations with constant coefficients. The solutions can be easily obtained by standard procedures for solving linear differential equations, and they are

$$\bar{U}_{n0}(\phi)=B_1\sin(\lambda+1)\phi-B_2\cos(\lambda+1)\phi+\gamma B_3\sin(\lambda-1)\phi-\gamma B_4\cos(\lambda-1)\phi \tag{16a}$$

$$\bar{W}_{n0}(\phi)=B_1\cos(\lambda+1)\phi+B_2\sin(\lambda+1)\phi+B_3\cos(\lambda-1)\phi+B_4\sin(\lambda-1)\phi \tag{16b}$$

where $\gamma=(-3+\lambda+4\upsilon)/(3+\lambda-4\upsilon)$, and B_i $(i=1,2,3,4)$ are coefficients to be determined from boundary conditions.

In a brief summary, the solutions of Eqs. (5) are

$$u(\rho,\theta,\phi)=\sum_n\rho^\lambda[\cos\phi\bar{U}_{n0}(\phi)-\sin\phi\bar{W}_{n0}(\phi)]\cos n\theta+O(\rho^{\lambda+1})=\tilde{u}(\rho,\theta,\phi)+O(\rho^{\lambda+1}) \tag{17a}$$

$$v(\rho,\theta,\phi)=\sum_n\rho^\lambda(A_1\cos\lambda\phi+A_2\sin\lambda\phi)\sin n\theta+O(\rho^{\lambda+1})=\tilde{v}(\rho,\theta,\phi)+O(\rho^{\lambda+1}) \tag{17b}$$

$$w(\rho,\theta,\phi)=\sum_n\rho^\lambda[-\sin\phi\bar{U}_{n0}(\phi)-\cos\phi\bar{W}_{n0}(\phi)]\cos n\theta+O(\rho^{\lambda+1})=\tilde{w}(\rho,\theta,\phi)+O(\rho^{\lambda+1}) \tag{17c}$$

where $\bar{U}_{n0}(\phi)$ and $\bar{W}_{n0}(\phi)$ are given in Eqs. (16a) and (16b), and $O(\rho^{\lambda+1})$ are terms of higher order in ρ.

Boundary Conditions, Characteristic Equations, and Corner Functions

Having solutions to the equilibrium equations, attention is now turned to the boundary conditions along the edges of the sharp corner. These surfaces, $\phi=0$ and $\phi=\alpha$ (see Fig. 2) may each be either free or fixed. For example, for $\phi=\alpha$

(a) Free (traction forces are equal to zero)

$$T_r=\sigma_r\sin\alpha+\tau_{rz}\cos\alpha=0,$$
$$T_z=\tau_{zr}\sin\alpha+\sigma_z\cos\alpha=0,$$
$$T_\theta=\tau_{\theta r}\sin\alpha+\tau_{\theta z}\cos\alpha=0 \tag{18a}$$

(b) Fixed

$$u(\rho,\theta,\alpha)=v(\rho,\theta,\alpha)=w(\rho,\theta,\alpha)=0 \tag{18b}$$

Substituting the displacements (Eqs. (17)) into Eqs. (2)–(4), as ρ approaches to zero, the singular stress components can be asymptotically expressed for each Fourier component (n) as

$$\sigma_r=\frac{\upsilon E}{(1+\upsilon)(1-2\upsilon)}\Lambda+\frac{E}{1+\upsilon}\left(\tilde{u}_{,\rho}\cos\phi-\frac{\sin\phi\,\tilde{u}_{,\phi}}{\rho}\right)+O(\rho^\lambda) \tag{19a}$$

Table 1 Characteristic equations and corner functions for all combinations of fixed or free intersecting surface

Boundary conditions			
$\phi=0$	$\phi=\alpha$	Characteristic equations	Corner functions
Free	Free	$\sin\lambda\alpha=0$ $\sin\lambda\alpha=\pm\lambda\sin\alpha$	$\nu=\rho^{\lambda}\cos\lambda\phi\sin n\theta$ $u=\rho^{\lambda}(\cos\phi U_1-\sin\phi W_1)\cos n\theta$ $w=\rho^{\lambda}(-\sin\phi U_1-\cos\phi W_1)\cos n\theta$
Free	Fixed	$\cos\lambda\alpha=0$ $\sin^2\lambda\alpha=\dfrac{4(-1+\upsilon)^2-\lambda^2\sin^2\alpha}{3-4\upsilon}$	$\nu=\rho^{\lambda}\cos\lambda\phi\sin n\theta$ $u=\rho^{\lambda}(\cos\phi U_2-\sin\phi W_2)\cos n\theta$ $w=\rho^{\lambda}(-\sin\phi U_2-\cos\phi W_2)\cos n\theta$
Fixed	Fixed	$\sin\lambda\alpha=0$ $\sin\lambda\alpha=\pm\dfrac{\lambda\sin\alpha}{3-4\upsilon}$	$\upsilon=\rho^{\lambda}\sin\lambda\phi\sin n\theta$ $u=\rho^{\lambda}(\cos\phi U_3-\sin\phi W_3)\cos n\theta$ $w=\rho^{\lambda}(-\sin\phi U_3-\cos\phi W_3)\cos n\theta$

Note:
$U_1=-(-1+\lambda)/(3+\lambda-4\upsilon)\eta_1\sin(\lambda+1)\phi+(1+\lambda)/(3+\lambda-4\upsilon)\cos(\lambda+1)\phi-\gamma\eta_1\sin(\lambda-1)\phi-\gamma\cos(\lambda-1)\phi$,
$W_1=-(-1+\lambda)/(3+\lambda-4\upsilon)\eta_1\cos(\lambda+1)\phi-(1+\lambda)/(3+\lambda-4\upsilon)\sin(\lambda+1)\phi-\eta_1\cos(\lambda-1)\phi+\sin(\lambda-1)\phi$,
$U_2=-(-1+\lambda)/(3+\lambda-4\upsilon)\eta_2\sin(\lambda+1)\phi+(1+\lambda)/(3+\lambda-4\upsilon)\cos(\lambda+1)\phi+\gamma\,\eta_2\sin(\lambda-1)\phi-\gamma\cos(\lambda-1)\phi$,
$W_2=-(-1+\lambda)/(3+\Lambda-4\Upsilon)\eta_2\cos(\lambda+1)\phi-(1+\lambda)/(3+\lambda-4\upsilon)\sin(\lambda+1)\phi+\eta_2\cos(\lambda-1)\phi+\sin(\lambda-1)\phi$,
$U_3=-\eta_3\sin(\lambda+1)\phi+(-3+\lambda+4\upsilon)/(3+\lambda-4\upsilon)\cos(\lambda+1)\phi+\gamma\eta_3\sin(\lambda-1)\phi-\gamma\cos(\lambda-1)\phi$,
$W_3=-\eta_3\cos(\lambda+1)\phi-(-3+\lambda+4\upsilon)/(3+\lambda-4\upsilon)\sin(\lambda+1)\phi+\eta_3\cos(\lambda-1)\phi+\sin(\lambda-1)\phi$,
$\eta_1=[\lambda\sin(\lambda-2)\alpha-(2+\lambda)\sin\lambda\alpha]/[2\lambda\sin\alpha\sin(\lambda-1)\alpha]$, $\eta_2=[2(-1+\upsilon)\cos\alpha\cos\lambda\alpha+(-1+\lambda+2\upsilon)\sin\alpha\sin\lambda\alpha]/[(-2+\lambda+2\upsilon)\sin\alpha\cos\lambda\alpha+(1-2\upsilon)\cos\alpha\sin\lambda\alpha]$,
$\eta_3=[-\gamma[\cos(\lambda+1)\alpha-\cos(\lambda-1)\alpha]]/[-\sin(\lambda+1)\alpha+\gamma\sin(\lambda-1)\alpha]$.

$$\sigma_z=\frac{\upsilon E}{(1+\upsilon)(1-2\upsilon)}\Lambda+\frac{E}{1+\upsilon}\left(-\sin\phi\tilde{w}_{,\rho}-\frac{\cos\phi\tilde{w}_{,\phi}}{\rho}\right)+O(\rho^{\lambda}) \tag{19b}$$

$$\sigma_\theta=\frac{\upsilon E}{(1+\upsilon)(1-2\upsilon)}\Lambda+O(\rho^{\lambda}) \tag{19c}$$

$$\tau_{r\theta}=\tau_{\theta r}=\frac{E}{2(1+\upsilon)}\left(\cos\phi\tilde{\upsilon}_{,\rho}-\frac{\sin\phi\tilde{\upsilon}_{,\phi}}{\rho}\right)+O(\rho^{\lambda}) \tag{19d}$$

$$\tau_{z\theta}=\tau_{\theta z}=\frac{E}{2(1+\upsilon)}\left(-\sin\phi\tilde{\upsilon}_{,\rho}-\frac{\cos\phi\tilde{\upsilon}_{,\phi}}{\rho}\right)+O(\rho^{\lambda}) \tag{19e}$$

$$\tau_{rz}=\tau_{zr}=\frac{E}{2(1+\upsilon)}\left(\cos\phi\tilde{w}_{,\rho}-\frac{\sin\phi\tilde{w}_{,\phi}}{\rho}-\sin\phi\tilde{u}_{,\rho}-\frac{\cos\phi\tilde{u}_{,\phi}}{\rho}\right)+O(\rho^{\lambda}) \tag{19f}$$

where $\Lambda=\cos\phi\tilde{u}_{,\rho}-\dfrac{\sin\phi\tilde{u}_{,\phi}}{\rho}-\sin\phi\tilde{w}_{,\rho}-\dfrac{\cos\phi\tilde{w}_{,\phi}}{\rho}$.

Substituting either the displacements of Eqs. (17), or the stresses of Eqs. (19), as needed, into the boundary conditions of either Eq. (18*a*) or (18*b*) at the faces $\phi=0$ and $\phi=\alpha$ yields six homogeneous, linear algebraic equations in the six coefficients A_1, A_2, B_1, B_2, B_3, and B_4. For a nontrivial solution the determinant of the coefficient matrix is set to zero, from which the eigenvalues (λ) are obtained. Moreover, the coefficients A_1 and A_2 are uncoupled from the remaining four, so two sets of λ are determined, one set from the second order determinant of A_1 and A_2, and one set from the fourth order (B_1,B_2,B_3,B_4) determinant.

For example, if the surface $\phi=0$ and $\phi=\alpha$ are both fixed, then one obtains from the second of Eqs. (18*b*)

$$\begin{bmatrix}\cos\lambda\alpha & \sin\lambda\alpha\\ 1 & 0\end{bmatrix}\begin{Bmatrix}A_1\\ A_2\end{Bmatrix}=0 \tag{20}$$

Whence $\sin\lambda\alpha=0$ is the characteristic equation for this set of λ. Applying the first and third of Eqs. (18*b*) at $\phi=0$ and $\phi=\alpha$ results in a set of four equations

$$\begin{bmatrix}0 & 1 & 0 & \gamma\\ 1 & 0 & 1 & 0\\ \sin(\lambda+1)\alpha & -\cos(\lambda+1)\alpha & \gamma\sin(\lambda-1)\alpha & -\gamma\cos(\lambda-1)\alpha\\ \cos(\lambda+1)\alpha & \sin(\lambda+1)\alpha & \cos(\lambda-1)\alpha & \sin(\lambda-1)\alpha\end{bmatrix}\times\begin{Bmatrix}B_1\\ B_2\\ B_3\\ B_4\end{Bmatrix}=0 \tag{21}$$

Evaluating the determinant, using some trigonometric identities, and simplifying it further, one arrives at

$$\sin\lambda\alpha=\pm\frac{\lambda\sin\alpha}{3-4\upsilon} \tag{22}$$

Having the characteristic equations, the eigenvalues λ can be determined from them and substituted into Eqs. (20) and (21) to obtain the eigenvectors A_1/A_2 and B_1/B_4, B_2/B_4, B_3/B_4. The resulting eigenfunctions are the desired corner functions, having arbitrary amplitudes which may be taken as unity.

The characteristic equations for all three combinations of fixed or free corner surfaces have been obtained. They are given in Table 1. The equations corresponding to u and w in Table 1 were obtained by Zak [27] for the axisymmetric ($n=0$) case only, using a different approach. These equations are also identical to those derived by Williams [1] for the sharp corner plane elasticity problems.

The corner functions for the three combinations of fixed or free edges are also presented in Table 1. They have not been found in the previously published literature.

Equations (19*d*) and (19*e*) show that the shear stresses $\tau_{r\theta} = \tau_{\theta r}$ and $\tau_{z\theta} = \tau_{\theta z}$ depend only on v, whereas the other stresses depend upon u and w. Because the characteristic equations for v are different from those for u and w, the singularities for the former stresses are different from those for the latter ones.

Concluding Remarks

The objective of this work was to derive corner displacement functions (u,v,w) which represent well the stresses and deformation of an elastic body of revolution in the vicinity of a sharp boundary corner. This was accomplished by means of an asymptotic analysis, which resulted in the characteristic equations and their corresponding corner functions summarized in Table 1.

The corner functions will be used in future 3D studies to determine accurate free vibration frequencies and mode shapes of bodies having such boundary discontinuities. These occur frequently in practice when rods or bars are machined (e.g., a circumferential V notch, or an abrupt diameter change). Although other corner functions have been used to advantage for vibration studies of 2D continuous systems [13–16,18], and the present ones are expected to be suitable for 3D vibration problems, they can also be used for static stress and deformation analysis, especially for determining the stress intensity factors for a V notch.

The present work deals with single homogeneous bodies. It would also be useful to have corner functions for bimaterial bodies, such as when a truncated cone is bonded to a cylinder of other material, as shown in Fig. 1. This will be the subject of a future study.

References

[1] Williams, M. L., 1952, "Stress Singularities Resulting from Various Boundary Conditions in Angular Corners of Plates in Extension," Am. J. Sci., **19**, pp. 526–528.
[2] Williams, M. L., 1953, "Discussion of 'Stress Singularities Resulting from Various Boundary Conditions in Angular Corners of Plates in Extension'," Am. J. Sci., **20**, pp. 590.
[3] Williams, M. L., 1952, "Surface Stress Singularities Resulting from Various Boundary Conditions in Angular Corners of Plates under Bending," *Proceedings of the First U.S. National Congress of Applied Mechanics*, ASME, New York, pp. 325–329.
[4] Sih, G. C., and Rice, J. R., 1964, "The Bending of Plates of Dissimilar Materials with Cracks," Am. J. Sci., **31**, pp. 477–482.
[5] Hein, V. L., and Erdogan, F., 1971, "Stress Singularities in a Two-Material Wedge," Int. J. Fract. Mech., **7**, pp. 317–330.
[6] Bogy, D. B., and Wang, K. C., 1971, "Stress Singularities at Interface Corners in Bonded Dissimilar Isotropic Elastic Materials," Int. J. Solids Struct., **7**, pp. 993–1005.
[7] Ting, T. C. T., 1990, "Interface Cracks in Anisotropic Bimaterials," J. Mech. Phys. Solids, **38**, pp. 505–513.
[8] Hartranft, R. J., and Sih, G. C., 1969, "The Use of Eigenfunction Expansions in the General Solution of the Three-Dimensional Crack Problems," J. Math. Mech., **19**, pp. 123–138.
[9] Su, X. M., and Sun, C. T., 1996, "On Singular Stress at the Crack Tip of a Thick Plate Under In-Plane Loading," Int. J. Fract., **82**, pp. 237–252.
[10] Glushkov, E., Glushkova, N., and Lapina, O., 1999, "3-D Elastic Stress Singularity at Polyhedral Corner Points," Int. J. Solids Struct., **36**, pp. 1105–1128.
[11] Ritz, W., 1908, "Über eine neue Methode zur Lösung gewisser Variationsprobleme der mathematischen Physik," J. Reine Angew. Math., **135**, pp. 1–61.
[12] Ritz, W., 1909, "Theorie der Transversalschwingungen einer quadratische Platte mit freien Rändern," Ann. Phys., **28**, pp. 737–786.
[13] Leissa, A. W., McGee, O. G., and Huang, C. S., 1993, "Vibrations of Sectorial Plates Having Corner Stress Singularities," Am. J. Sci., **60**, pp. 134–140.
[14] Leissa, A. W., McGee, O. G., and Huang, C. S., 1993, "Vibrations of Circular Plates Having V-Notches or Sharp Radial Cracks," J. Sound Vib., **161**, pp. 227–239.
[15] McGee, O. G., Leissa, A. W., and Huang, C. S., 1992, "Vibrations of Cantilevered Skew Plates with Corner Stress Singularities," Int. J. Numer. Methods Eng., **35**, pp. 409–423.
[16] Huang, C. S., McGee, O. G., Leissa, A. W., and Kim, J. W., 1995, "Accurate Vibration Analysis of Simply Supported Rhombic Plates by Considering Stress Singularities," ASME J. Vibr. Acoust., **117**, pp. 245–251.
[17] Huang, C. S., 2003, "Stress Singularities in Angular Corners in First-Order Shear Deformation Plate Theory," Int. J. Mech. Sci., **45**, pp. 1–20.
[18] Huang, C. S., Leissa, A. W., and Chang, M. J., 2005, "Vibrations of Skewed Cantilevered Triangular, Trapezoidal and Parallelogram Mindlin Plates with Considering Corner Stress Singularities," Int. J. Numer. Methods Eng., **62**, pp. 1789–1806.
[19] Yosibash, Z., and Schiff, B., 1993, "A Superelement for Two-Dimensional Singular Boundary Value Problems in Linear Elasticity," Int. J. Fract., **62**, pp. 325–340.
[20] Belytschko, T., Krongauz, Y., Fleming, M., Organ, D., and Liu, W. K., 1996, "Smoothing and Accelerated Computations in the Element Free Galerkin Method," J. Comput. Appl. Math., **74**, pp. 111–126.
[21] Fleming, M., Chu, Y. A., Moran, B., and Belyschko, T., 1997, "Enriched Element Free Galerkin Methods for Crack Tip Fields," Int. J. Numer. Methods Eng., **40**, pp. 1483–1504.
[22] Dolbow, J., Möse, N., and Belyschko, T., 2000, "Discontinuous Enrichment in Finite Element with a Partition of Unity Method," Finite Elem. Anal. Design, **36**, pp. 235–260.
[23] Leissa, A. W., and So, J., 1995, "Comparisons of Vibration Frequencies of Rods and Beams from One-Dimensional and Three-Dimensional Analyses," J. Acoust. Soc. Am., **98**, pp. 2122–2135.
[24] Leissa, A. W., and So, J., 1995, "Three-Dimensional Vibrations of Truncated Hollow Cones," J. Vib. Control, **1**, pp. 145–158.
[25] Leissa, A. W., and Kang, J.-H., 1999, "Three-Dimensional Vibration Analysis of Thick Shells of Revolution," J. Engrg. Mech. Div., **125**, pp. 1365–1372.
[26] Leissa, A. W., and Kang, J.-H., 2000, "Three-Dimensional Vibrations of Thick Spherical Shell Segments with Variable Thickness," Int. J. Solids Struct., **37**, pp. 4811–4823.
[27] Zak, A. R., 1964, "Stresses in the Vicinity of Boundary Discontinuities in Bodies of Revolution," Am. J. Sci., **31**, pp. 150–152.
[28] Love, A. E. H., 1927, *A Treatise on the Mathematical Theory of Elasticity*, 4th ed., The Macmillan Co, New York (reprinted by Daver Publications, 1944).
[29] Sokolnikoff, I. S., 1956, *Mathematical Theory of Elasticity*, 2nd ed., McGraw-Hill Book, New York.
[30] Chaudhuri, R. A., and Xie, M., 2000, "A Novel Eigenfunction Expansion Solution for Three-Dimensional Crack Problems," Compos. Sci. Technol., **60**, pp. 2565–2580.